

Use of Stopped-Flow Fluorescence Spectroscopy to Measure Rapid Membrane Binding by Protein Kinase C

Eric A. Nalefski and Alexandra C. Newton

1. Introduction

In investigating the binding of ligands to proteins, many studies have been concerned with answering the fundamental questions proposed by Scatchard (*1*), that is, “How many” and “How tightly bound?” Although these questions are of utmost importance, the kineticist also wishes to know “How rapidly?” The development of rapid kinetic methodologies has provided many of the tools to answer the latter question (*2–4*). Suitably designed kinetic experiments may, in many instances, be able to provide answers to the former questions as well. Moreover, kinetic studies may yield mechanistic insight that cannot be elucidated from other approaches.

The appearance and disappearance of transient second messengers during cell signal transduction places rigid constraints on the kinetic rate constants of signaling proteins that bind them. The time course of binding and release of these messengers must match their rise and fall to ensure that these signaling proteins serve as effective “on-off” switches. These constraints appear to operate on conventional isoforms of protein kinase C (PKC), a molecular sensor that translocates to cellular membranes and is activated upon binding two second messengers, Ca^{2+} and diacylglycerol (DG) (*5*). Levels of both these signaling molecules transiently rise during cellular activation and then fall to a resting state (*6,7*). Binding of Ca^{2+} to the PKC C2 domain triggers its engagement with anionic phospholipids (*8*). Full activation of the enzyme, however, requires additional contact with the membrane through binding of its

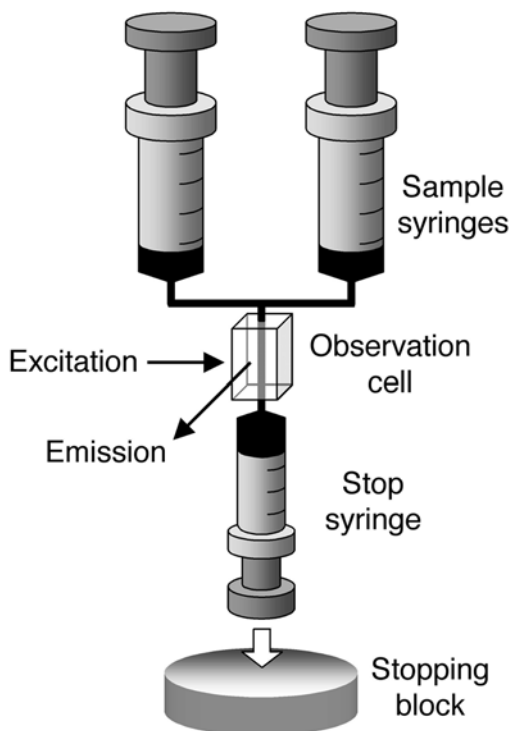


Fig. 1. Schematic of the stopped-flow apparatus and mechanism. Syringes containing two sample solutions are compressed, forcing the mixing of the reactants and their entry into an observation cell. The contents of the observation cell, consisting of the previous reaction solution, are forced out and pass into the stop syringe, whose plunger hits the stopping block, terminating the mixing process. The progress of the reaction is monitored in the observation cell using excitation light and emission measured at right angles to the excitation beam.

C1 domain(s) to membrane-sequestered DG and stereoselective recognition of phosphatidylserine (5).

This chapter will provide strategies for determining the rate constants for binding of PKC and its isolated regulatory domains to synthetic phospholipid vesicles using rapid stopped-flow fluorescence spectroscopy. This technique measures the observed rate of binding of two reactants, in this case, protein and phospholipid vesicles of defined size and composition, under pseudo first-order conditions. These reactants are rapidly mixed together by the action of a stop syringe (**Fig. 1**). The reaction is monitored by recording fluorescence changes in the reactants or products upon formation of products. By fitting the spectroscopic data to simple exponential equations, quantitative information

about the extent of binding, from the fluorescence amplitudes, and the observed rate of the approach to binding equilibrium (k_{obs}) is obtained. The dependence of k_{obs} on reactant concentrations for a simple one-step binding mechanism allows determination of kinetic constants k_{on} and k_{off} , from which the apparent dissociation constant (K_{d}) can be calculated ($K_{\text{d}} = k_{\text{off}}/k_{\text{on}}$). The dependence of the observed fluorescence change amplitude on reactant concentration provides an independent measure of the K_{d} value.

2. Materials

1. Several milliliters of purified protein in the micromolar range are required for the assay. Methods for purification of full-length PKC have been described (9) as have methods for production of recombinant PKC regulatory C2 and C1 domains as glutathione S-transferase fusion proteins expressed in *Escherichia coli* (8). Alternatively, His₆-fusion proteins for purification over nickel resins can be used (10).
2. Stocks of the phospholipids phosphatidylserine, phosphatidylcholine (PC), and DG are diluted in chloroform and stored at -20°C . Stock concentrations of commercial phospholipids should be determined as described below. Stocks of phorbol esters are diluted in dimethylsulfoxide and stored at -20°C . For the fluorescence resonance energy transfer (FRET) application (11), fluorescent or nonfluorescent acceptor phospholipids are required. A suitable fluorescence acceptor of tryptophans in proteins that bind phospholipid vesicles is *N*-(5-dimethylaminonaphthalene-1-sulfonyl)-1,2-dihexadecanoyl-*sn*-glycero-3-phosphoethanolamine (danysl PE or dPE) (12). Fluorescent phospholipid stocks are stored in the dark to avoid photobleaching. A method for preparing phospholipid vesicles of defined size by extrusion is described below. A visible light absorbance spectrophotometer is required for phospholipid quantification.
3. A stopped-flow fluorescence spectrophotometer capable of UV excitation and collecting and storing emission data is required. Hardware capable of reliably mixing together relatively small volumes ($<100\ \mu\text{L}$) will provide efficient use of samples. Because fluorescence is highly dependent on temperature, thermostatted chambers surrounding sample syringes and the observation cell are required to maintain constant temperature. Depending on the instrument, filters (cut-off or band pass) may be required to collect fluorescence emission at the desired wavelengths.
4. Computer software capable of rapid least-squares analysis of data using exponential equations is required (3). If possible, data can be analyzed directly by the software supplied with the stopped-flow apparatus. Alternatively, data may be processed using the method of global analysis (13).
5. Buffered solutions for the experiment must be individually optimized for the protein and should be free of detergents and fluorescent contaminants. Suitable buffers include HEPES, PIPES, MOPS, but not Tris. Phosphate buffers must not be used because they interfere with phospholipid quantification and are

incompatible with assays involving the addition of Ca^{2+} . Assay buffer consisting of 150 mM NaCl, 20 mM HEPES (pH 7.4), and 5 mM dithiothreitol has been successfully used with full-length PKC β II and its isolated C2 domain (**14**). Either ethylenediaminetetraacetic acid or Ca^{2+} may be included, depending on whether a Ca^{2+} -triggered binding event is being measured.

3. Methods

3.1. Protein Stock Preparation

Protein should be stored in buffers that stabilize protein activity. Protein stocks may be quantified using molar extinction coefficient and absorbance spectroscopy (**15**) or bichinonic acid using bovine serum albumin as a standard (**16**). Proteins must be able to survive the conditions of the assay for extended periods of time, for example, up to an hour at the temperature chosen. Immediately before use, proteins are rapidly thawed from frozen stocks maintained at -80°C , diluted into assay buffer, and kept on ice until analysis.

3.2. Phospholipid Vesicle Stock Preparation

Vesicles are prepared, as described in **Subheading 3.2.1.**, from mixtures of 20–40% PS, with the remaining phospholipid consisting of PC. Such vesicles have been used successfully with full-length PKC β II and its isolated C2 domain (**14**). For the FRET application, the anionic phospholipid dPE may be incorporated at 2–5%, and the PS composition is adjusted to maintain the desired percentage of total anionic phospholipid. The concentration of vesicles is determined by a modified phosphate assay (**17**), as described in **Subheading 3.2.2.**

3.2.1. Generation of Phospholipid Vesicles

1. Phospholipid stocks in chloroform are dispensed into glass test tubes, mixed, and dried down under a gentle stream of nitrogen gas into a thin transparent film.
2. Assay buffer is added to reconstitute phospholipids at approx 1–10 mM phospholipid.
3. The suspension is agitated vigorously by vortexing until a cloudy solution is formed and the film is completely removed from the sides of the tube.
4. The solution is transferred to a plastic vessel and subjected to at least three freeze-thaw cycles at -80°C and room temperature, respectively. Reconstituted phospholipids may be stored at -80°C until extrusion.
5. A suspension of 100-nm diameter vesicles is formed by extruding the thawed solution through double-stacked 100-nm pore size polycarbonate filters according to manufacturer's instructions.

3.2.2. Phospholipid Vesicle Quantification

1. A series of the unknown vesicles, ranging from 1 to 10 μL , and phosphate standards, ranging from 1 to 10 nmol (1 to 10 μL of 10 mM phosphate) are dispensed into disposable borosilicate glass test tubes along with a blank tube lacking phosphate.
2. 100 μL of 5 M sulfuric acid is added, and the mixture is heated to 150°C for at least 3 h.
3. 30 μL of 30% hydrogen peroxide (stored at 4°C) is added, and the mixture is heated to 150°C for an additional 90 min.
4. 920 μL of 0.22% ammonium molybdate and 50 μL of 10% ascorbic acid are added, and the mixture solution is heated to 100°C for 15 min.
5. Solutions are diluted fourfold into water, and absorbance is recorded at 830 nm.
6. After subtracting the blank value, measured from the reaction tube lacking phosphate, absorbance is plotted against the mass of the phosphate standard and the volume of the unknown. Slopes are determined using linear regression of data points in the linear range of the assay. The concentration of phosphate in the vesicle stock (in nmol per μL) is calculated by dividing its slope (in absorbance units per μL unknown) by the standard slope (in absorbance units per nmol phosphate). Phospholipid concentration is taken as the calculated phosphate concentration, from which vesicle concentration is calculated, assuming 90,000 phospholipids per vesicle of 100 nm diameter (18).

3.3. Sample Analysis

3.3.1. Sample Dilutions

A series of 2X vesicle solutions, 1–2 mL each, and a single protein solution, equal in volume to the total volume of vesicle solutions, are prepared in assay buffer immediately prior to analysis. The concentration of protein, generally 0.1–1 μM , required to provide an adequate fluorescence signal must be determined empirically. Vesicles are diluted over a wide range (e.g., 0.2–2.4 nM) gravimetrically. To assure pseudo first-order conditions of binding sites with respect to protein, the total concentration of target phospholipids must be in vast excess (at least 10-fold) of protein. Vesicles containing fluorescent phospholipids should be kept in the dark to avoid photobleaching.

3.3.2. Fluorometer Preparation

While the apparatus is allowed to equilibrate, stopped-flow plumbing lines and sample syringes are washed out extensively to remove any residual impurities from previous use. A good regimen would include successive washes with 10% SDS, 1 N NaOH, water, 1 N HCl, and then copious amounts of water. Finally, the plumbing lines are flushed extensively with assay buffer.

3.3.3. Instrument Settings

Because tryptophan emission varies considerably between proteins ($\lambda_{\text{max}} = 310\text{--}350\text{ nm}$), intrinsic tryptophan fluorescence may be monitored using 280 nm excitation and collecting emission with a 325 nm high-pass filter. For the FRET application, tryptophan is excited using 280 nm light and dPE emission is recorded using a 475 nm high-pass filter.

Although other instrument settings must be optimized carefully for each fluorescence application and instrument, certain guidelines may be followed; these are detailed in **ref. 3**. For instance, voltage and gain settings must be optimized for each application to achieve suitable signal to noise ratios. Excitation and emission slit widths should be adjusted, for example, to $\leq 5\text{ nm}$, to allow sufficient light detection without photobleaching of sensitive materials. For short time collections ($< 1\text{ s}$), pressure should be maintained on the stop syringe during data collection, if possible, to avoid artifacts caused by abrupt pressure changes. To conserve sample materials, the stopped-syringe settings should be adjusted to minimize the mixing volume without compromising the ability of the mechanism to flush out the contents of the previous reaction from the observation cell.

3.3.4. Data Collection

Protein solution is applied to one sample syringe, and the series of vesicle dilutions are applied, beginning with the lowest vesicle concentration, to the other. This approach obviates washing out the lines after application of a new vesicle stock. Samples are allowed to equilibrate to the thermostatted temperature for 5 min before collecting data. Individual test traces must be collected after application of a new vesicle stock to establish when the plumbing lines are completely cleared of previous reaction mixtures. For each time course, 1000–2000 data points are collected. Five such time courses are collected and averaged together, and then three sets of these averaged experiments are collected. If possible, each trace should be viewed prior to averaging so that aberrant traces, if any, can be omitted. The time base required for each experiment must be determined iteratively: a test run is analyzed to estimate the rate constant for the reaction, and then the final experiment is carried out at a collection time equal to five times the half-life to observe the reaction proceed to 97% completion (*see Note 1*).

3.4. Data Analysis

The goal of the kinetic approach presented here is to formulate the simplest mechanism that describes the steps in a binding reaction and to determine the observed rate constants for these steps. Analysis of the time courses described

presently is simplified by conducting the experiments under pseudo first-order conditions, which reduces the observable steps to one or more exponential processes. Hence, the primary data are first fitted with simple exponential equations to determine the number of slowest observable steps in the binding process. This analysis provides the observed pseudo first-order rate constants and amplitudes for each reactant concentration. The dependence of these rate constants on reactant concentrations is then determined to ascertain the forward and reverse rate constants, from which the dissociation constant can be calculated. The dependence of the observed amplitudes on reactant concentrations is determined to independently evaluate the dissociation constant.

The following will describe kinetic experimentation in which intrinsic tryptophan emission is recorded and the time-dependent changes in fluorescence intensity are analyzed to extract apparent rate and equilibrium constants. Nevertheless, this analysis procedure may be applied to primary FRET data as well (14).

3.4.1. Fitting Primary Fluorescence Data

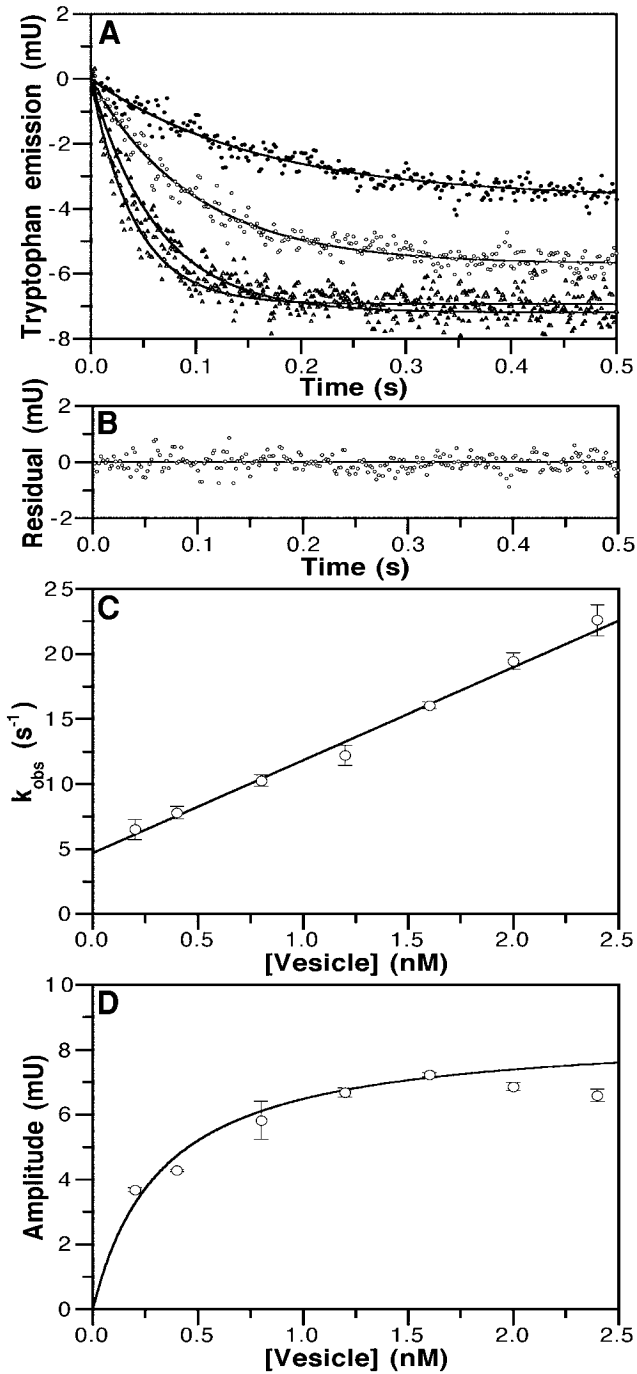
Only data collected beyond the experimental dead time, which must be determined empirically (see Note 2), are to be included in the data analysis. Using the method of least-squares analysis (19), the fluorescence intensities are fitted with exponential equations of the general form (3):

$$F(t) = F_0 + \sum_{i=1}^n A_{\text{obs}(i)} e^{-k_{\text{obs}(i)} t} \quad (1)$$

where $F(t)$ represents the observed fluorescence at time t , F_0 is a fluorescence offset representing the final fluorescence, $A_{\text{obs}(i)}$ represents the amplitude and $k_{\text{obs}(i)}$ is the observed rate constant for the i th of n phases. Time courses are first fitted with a monoexponential equation to test whether the binding process may be approximated by a simple bimolecular interaction between the reactants (see Note 3).

The fitted value of F_0 may be subtracted from $F(t)$ to display each time course as an “offset fluorescence” in arbitrary units (U), which runs from a value of 0 to A_{obs} (Fig. 2A). This is particularly useful because the parameter that best reflects fractional binding saturation at equilibrium is the magnitude of A_{obs} , not the final observed fluorescence, which may vary between experiments due to instrument drift. Alternatively, the progression to binding equilibrium in different binding reactions may be represented by dividing the offset fluorescence by A_{obs} to obtain time courses that proceed from 0 to 1.

Two straightforward tests for the adequacy of data fitting involve simple inspection of the fitted parameters and analysis of residual plots. The fitted



parameters must be reasonable (e.g., give rate constants that are consistent with the time base of data collection) and have small errors associated with them. For each vesicle concentration, residuals are calculated as the difference between $F(t)$ and $F_{\text{calc}(t)}$, the theoretical value based on the fitted parameters (see **Fig. 2B**). Residuals that are small and randomly distributed about zero are indicative of adequate fitting of the data.

The data are then fitted with biexponential equations to determine whether significant improvement in the fitting results (see **Note 4**). Caution is advised when judging the significance of the improvement in curve fitting by the addition of a second exponential term, since the inclusion of additional parameters almost always improves the performance of a given equation. Guidelines for ascertaining the “goodness of fit” are described in detail elsewhere (**2,20,21**).

3.4.2. Determining Apparent Forward and Reverse Rate Constants

For simple monophasic time courses representing the reversible binding of proteins to vesicles carried out under pseudo first-order conditions, the observed rate constants are plotted as a function of vesicle concentration (**Fig. 2C**). The data are fitted with a linear equation represented by **Eq. 2**:

$$k_{\text{obs}} = k_{\text{on}}[v] + k_{\text{off}} \quad (2)$$

Here, k_{on} (the slope) represents an apparent second-order association rate constant (in units of $M^{-1} s^{-1}$), and k_{off} (the y-intercept) represents an apparent first-order dissociation rate constant (in units of s^{-1}). Because three determina-

Fig. 2. (see facing page) Kinetics of PKC β II C1B domain binding to anionic phospholipid vesicles containing DG. Purified PKC β II C1B domain variant Y123W ($0.5 \mu M$) was rapidly mixed with an equal volume of solutions containing increasing concentration of DG-PS-PC (5:35:60) vesicles. Tryptophan was excited with 280 nm excitation light and emission was recorded with a 325 nm high-pass filter. **(A)** Representative traces showing time course of tryptophan emission decreases for C1B-Y123W domain mixed with 0.2, 0.8, 1.6, and 2.4 nM (final) vesicles (top to bottom). Solid lines show monoexponential fit with **Eq. 1**, which yielded k_{obs} and amplitude values. **(B)** Representative residual plot from monoexponential fit of time course taken from data employing 0.8 nM vesicles shown in A. **(C)** Dependence of k_{obs} on vesicle concentration. Bars indicate standard deviation of three determinations from a single experiment. Weighted least-squares analysis using **Eq. 2** revealed a slope value for k_{on} equal to $0.71 (\pm 0.03) \times 10^{10} M^{-1} s^{-1}$ and a y-intercept value for k_{off} equal to $4.7 (\pm 0.4) s^{-1}$. From these values, a K_d^{calc} equal to $0.66 (\pm 0.06) nM$ can be estimated. **(D)** Dependence of amplitude on vesicle concentration. Bars indicate standard deviation of three determinations from a single experiment. Weighted least-squares analysis using Equation 3 yielded a K_d^{obs} equal to $0.33 (\pm 0.02) nM$.

tions are performed for each vesicle concentration, the data should be weighted by the uncertainties in k_{obs} values (19). The ratio of the fitted parameters, k_{off} to k_{on} , provides the calculated apparent vesicle dissociation constant ($K_{\text{d}}^{\text{calc}}$, in units of M). For the more complex case of biphasic time courses generated by protein binding to vesicles, estimating the rate constants is more involved (see Note 5).

3.4.3. Determining Apparent Dissociation Constants

The observed amplitudes (A_{obs}) are plotted as a function of vesicle concentration and fitted with a hyperbolic equation represented by Eq. 3:

$$A_{\text{obs}} = A_{\text{max}} \left(\frac{[v]}{[v] + K_{\text{d}}^{\text{obs}}} \right) \quad (3)$$

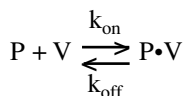
Here, A_{max} represents the calculated maximal amplitude and $K_{\text{d}}^{\text{obs}}$ represents the observed vesicle dissociation constant (see Fig. 2D). In cases where vesicle concentrations may be tested both well below and above the K_{d} value, $K_{\text{d}}^{\text{obs}}$ should agree reasonably well with the $K_{\text{d}}^{\text{calc}}$ value based on the measured kinetic constants.

4. Notes

1. Because the half-life ($t_{1/2}$) is equal to $\ln 2/k$, the amplitude at $t = 5t_{1/2}$ equals $A_{\text{obs}}e^{(-5\ln 2)}$, which in turn equals $0.03A_{\text{obs}}$.
2. A general method for determination of the mixing time of a stopped-flow apparatus is based on the reduction of 2,6-dichlorophenolindophenol (DCIP) by L-ascorbic acid (AA) (22), which can be followed spectroscopically. This procedure involves the determination of the dependence of the observed amplitude on the observed chemical reaction rate constant. A stock solution of 500 μM DCIP is prepared by dissolving 7.25 mg of DCIP into 5 mL of isopropanol containing 0.58 g NaCl, and the volume is raised to 50 mL with water. A 200 mM solution of AA is prepared by dissolving 0.88 g AA into 25 mL of an acid-salt solution comprised of 0.02 N HCl and 0.2 M NaCl. A series of AA dilutions, ranging from 2 to 100 mM, are then prepared in 3 mL of the acid-salt solution. Beginning with the lowest concentration, the AA solutions are rapidly mixed with the DCIP solution in the stopped-flow apparatus in absorbance mode, recording absorbance at 524 nm. The absorbance is plotted against time, and the average value observed within the first few milliseconds of each time course is noted. Because the absorbance of reduced DCIP is very small, this value represents ΔA_{obs} , the change in absorbance observable after mixing. Then, with the first several milliseconds masked, the data are fitted with monoexponential equations to obtain k_{obs} . Because the reaction is carried out under pseudo first-order conditions of AA with respect to DCIP, a plot of k_{obs} against AA concentration should yield a straight line. Because deviation from linearity is expected at high

AA concentrations, where reactions are completed within the mixing time, only those rate constants in the linear range are considered further. The $\ln(\Delta A_{\text{obs}})$ is plotted as a function of k_{obs} , and the absolute value of the resulting slope is taken as the dead time. The inverse natural log of the y-intercept represents the theoretic amplitude of the reaction, that is, the absorbance change that results from complete reduction of DCIP by AA under these conditions.

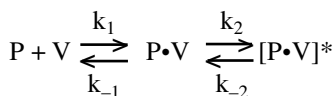
3. The simple bimolecular interaction may be represented by **Scheme I**:



Scheme I

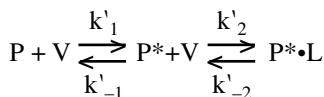
where P represents protein, V represents the phospholipid vesicle, and P•V represents the protein-vesicle complex.

4. Significantly improved fitting with biexponential equations suggests that the binding process involves two phases, which may be represented either by **Scheme II**:



Scheme II

or by **Scheme III**:



Scheme III

Scheme II illustrates a mechanism whereby the bimolecular interaction between protein and vesicle is then followed by a unimolecular isomerization of the P•V complex. In contrast, **Scheme III** shows how unimolecular isomerization of the protein (or the vesicle) may precede its binding to vesicles. Because either may take place, in principle, neither mechanism may be excluded solely on the basis of analysis of apparent rate constants (3).

5. For **Scheme II**, based on equations derived for general two-step mechanisms (3), the following approximations for the two phases are shown in **Eqs. 4 and 5**:

$$k_{\text{obs}(1)} \approx k_1[V] + k_{-1} + k_2 + k_{-2} \tag{4}$$

$$k_{\text{obs}(2)} \approx \left(\frac{k_1[V](k_2 + k_{-2}) + k_{-1}k_{-2}}{k_1[V] + k_{-1} + k_2 + k_{-2}} \right) \tag{5}$$

The $k_{\text{obs}(1)}$ values for the fast phase are plotted as a function of vesicle concentration and fitted with a linear equation represented by **Eq. 6**:

$$k_{\text{obs}(1)} = k_1[v] + C \quad (6)$$

In this case, k_1 (the slope) represents the apparent second-order rate constant for a bimolecular step. C (the y-intercept) represents the sum $k_{-1} + k_2 + k_{-2}$, where k_{-1} equals the apparent dissociation rate constant for the bimolecular step and $k_2 + k_{-2}$ is the sum of the forward and reverse rate constants for a first-order transition step. For the slow phase, $k_{\text{obs}(2)}$ is plotted as a function of vesicle concentration and fitted with a hyperbolic equation represented by **Eq. 7**:

$$k_{\text{obs}(2)} = k_{\text{max}(2)} \left(\frac{[v]}{[v] + C} \right) \quad (7)$$

where C is a constant and $k_{\text{max}(2)}$ represents the calculated asymptote, which is equal to the sum $k_2 + k_{-2}$. Hence, the difference in the y-intercept (**Eq. 4**) and the asymptote (**Eq. 5**) yields an estimate for k_{-1} . Estimates for the remaining rate constants k_2 and k_{-2} can in certain circumstances be determined by application of a trapping experiment (**14,23**). Different approaches have been used to determine these constants in other binding systems (**24,25**).

For the alternative **Scheme III**, the two phases are approximated by rearrangement of **Eqs. 4** and **5 (3)**:

$$k'_{\text{obs}(1)} \approx k'_1 + k'_{-1} + k'_2 [v] + k'_{-2} \quad (8)$$

$$k'_{\text{obs}(2)} \approx \frac{k'_1 (k'_2 [v] + k'_{-2}) + k'_{-1} k'_{-2}}{k'_1 + k'_{-1} + k'_2 [v] + k'_{-2}} \quad (9)$$

Here, $k'_{\text{obs}(1)}$ values are plotted as a function of vesicle concentration and fitted with a linear equation given by **Eq. 10**:

$$k'_{\text{obs}(1)} = k'_2 [v] + C' \quad (10)$$

where the slope represents the apparent second-order rate constant k'_2 and the y-intercept C' represents the sum $k'_1 + k'_{-1} + k'_{-2}$. For the slow phase, $k'_{\text{obs}(2)}$ is plotted as a function of vesicle concentration and fitted with a hyperbolic equation represented by **Eq. 11**:

$$k'_{\text{obs}(2)} = k'_{\text{max}(2)} \left(\frac{[v]}{[v] + C'} \right) \quad (11)$$

where C' is a constant and $k'_{\text{max}(2)}$ represents the calculated asymptote, which is equal to k'_1 . As before, estimates for the remaining constants k'_{-2} and k'_{-1} can be elucidated in certain circumstances from a trapping experiment (**14**).

Acknowledgment

This work was supported by NIH GM43154.

References

1. Scatchard, G. (1949) The attractions of proteins for small molecules and ions. *Ann. N. Y. Acad. Sci.* **51**, 660–672.
2. Johnson, K. A. (1986) Rapid kinetic analysis of mechanochemical adenosinetriphosphatases. *Methods Enzymol.* **134**, 677–705.
3. Johnson, K. A. (1992) Transient-state kinetic analysis of enzyme reaction pathways in *The Enzymes*, 3rd ed, Vol. 20 (Sigman, D. S., ed.), Harcourt Brace Jovanovich, San Diego, pp. 1–60.
4. Gutfreund, H. (1999) Rapid-flow techniques and their contributions to enzymology. *Trends Biochem. Sci.* **24**, 457–460.
5. Newton, A. C. and Johnson, J. E. (1998) Protein kinase C: a paradigm for regulation of protein function by two membrane-targeting modules. *Biochim. Biophys. Acta* **1376**, 155–172.
6. Berridge, M. J. (1990) Calcium oscillations. *J. Biol. Chem.* **265**, 9583–9586.
7. Werner, M. H., Bielawska, A. E., and Hannun, Y. A. (1992) Multiphasic generation of diacylglycerol in thrombin-activated human platelets. *Biochem. J.* **282**, 815–820.
8. Johnson, J. E., Giorgione, J., and Newton, A. C. (2000) The C1 and C2 domains of protein kinase C are independent membrane targeting modules, with specificity for phosphatidylserine conferred by the C1 domain. *Biochemistry* **39**, 11,360–11,369.
9. Orr, J. W. and Newton, A. C. (1992) Interaction of protein kinase C with phosphatidylserine. 1. Cooperativity in lipid binding. *Biochemistry* **31**(19), 4661–4667.
10. Ananthanarayanan, B., Das, S., Rhee, S. G., Murray, D., and Cho, W. (2002) Membrane targeting of C2 domains of phospholipase C- δ isoforms. *J. Biol. Chem.* **277**, 3568–3575.
11. Nalefski, E. A. and Falke, J. J. (2002) Use of fluorescence resonance energy transfer to monitor Ca²⁺-triggered membrane docking of C2 domains. *Methods Mol. Biol.* **172**, 295–303.
12. Bazzi, M. D. and Nelsestuen, G. L. (1987) Association of protein kinase C with phospholipid vesicles. *Biochemistry* **26**, 115–122.
13. Beechem, J. M. (1992) Global analysis of biochemical and biophysical data. *Methods Enzymol.* **210**, 37–53.
14. Nalefski, E. A. and Newton, A. C. (2001) Membrane binding kinetics of protein kinase C β II mediated by the C2 domain. *Biochemistry* **40**, 13,216–13,229.
15. Gill, S. C. and von Hippel, P. H. (1989) Calculation of protein extinction coefficients from amino acid sequence data. *Anal. Biochem.* **182**(2), 319–326.

16. Smith, P. K., Krohn, R. I., Hermanson, G. T, and Klenk, D. C. (1985) Measurement of protein using bicinchoninic acid. *Anal. Biochem.* **150**, 76–85.
17. Bartlett, G. R. (1958) Phosphorus assay in column chromatography. *J. Biol. Chem.* **234**, 466–468.
18. Arbuzova, A., Wang, J., Murray, D., Jacob, J., Cafiso, D. S., and McLaughlin, S. (1997). Kinetics of interaction of the myristoylated alanine-rich C kinase substrate, membranes, and calmodulin. *J. Biol. Chem.* **272**, 27,167–27,177.
19. Taylor, J. R. (1997) *An Introduction to Error Analysis*, 2nd ed, University Science Books, Sausalito, CA.
20. Mannervik, B. (1982). Regression analysis, experimental error, and statistical criteria in the design and analysis of experiments for discrimination between rival kinetic models. *Methods Enzymol.* **87**, 370–390.
21. Straume, M. and Johnson, M. L. (1992) Analysis of residuals: criteria for determining goodness-of-fit. *Methods Enzymol.* **210**, 87–105.
22. Tonomura, B., Nakatani, H., Ohnishi, M., Yamaguchi-Ito, J., and Hiromi, K. (1978) Test reactions for a stopped-flow apparatus. Reduction of 2,6-dichlorophenol-indophenol and potassium ferricyanide by L-ascorbic acid. *Anal. Biochem.* **84**, 370–383.
23. Torok, K. and Trentham, D. R. (1994) Mechanism of 2-chloro-(ϵ -amino-Lys75)-[6-[4-(N,N- diethylamino)phenyl]-1,3,5-triazin-4-yl]calmodulin interactions with smooth muscle myosin light chain kinase and derived peptides. *Biochemistry* **33**, 12,807–12,820.
24. Zhao, Z., Rothery, R. A., and Weiner, J. H. (1999) Stopped-flow studies of the binding of 2-n-heptyl-4-hydroxyquinoline-N-oxide to fumarate reductase of *Escherichia coli*. *Eur. J. Biochem.* **260**, 50–56.
25. Lacourciere, K. A., Stivers, J. T., and Marino, J. P. (2000) Mechanism of neomycin and Rev peptide binding to the Rev responsive element of HIV-1 as determined by fluorescence and NMR spectroscopy. *Biochemistry* **39**, 5630–5641.